

TEMPORAL CHANGES IN PEG HYDROGEL STRUCTURE INFLUENCE HUMAN MESENCHYMAL STEM CELL PROLIFERATION AND MATRIX MINERALIZATION

Charles R Nuttelman¹, April M Kloxin¹, and Kristi S Anseth^{1,2}

10.1. INTRODUCTION

Preventing bone resorption or facilitating bone regeneration are major clinical challenges for several dental procedures, including ridge preservation after tooth extractions, integration of tooth implants, and the treatment of severe periodontal disease^{1,2}. Many of the current treatments fail because of the inability of the materials and methods to heal osseous defects. Thus, recent directions in tissue engineering suggest strategies to design synthetic carriers for cell-based therapies that are targeted towards bone regeneration. For example, several groups³⁻⁵ are interested in the development of injectable gel carriers that would allow simple and reproducible clinical delivery of human mesenchymal stem cells (hMSCs) to treat bone defects. From a bone tissue engineering perspective, hMSCs have many advantages. A large number of hMSCs can be easily obtained by aspiration of adult bone marrow⁶, and these multipotent cells can then be coaxed to differentiate into osteoblasts by exposure to specific growth factors or hormones at the right time and with the right dose (e.g., dexamethasone, BMPs, others)⁷⁻⁹. During their differentiation to osteoblasts, hMSCs secrete significant amounts of extracellular matrix molecules, providing further advantages for tissue regeneration. Because of these properties, numerous groups are exploring the development of hydrogels for three-dimensional culture and expansion of hMSCs; controlled differentiation of hMSCs to osteoblasts¹⁰, chondrocytes¹¹, and other cell types¹²; and the targeted delivery of hMSCs to bone defects¹³.

¹Department of Chemical and Biological Engineering, University of Colorado, Boulder, Colorado, USA

²Howard Hughes Medical Institute, University of Colorado, Boulder, Colorado, USA

Hydrogels are desirable cell carriers for numerous applications because of their high water content, which imparts unique properties with respect to biocompatibility, transport, and elasticity. We are particularly interested in hydrogels formed from the photoinitiated chain polymerization of macromolecular poly(ethylene glycol) (PEG) monomers. These covalently crosslinked PEG hydrogels provide passive support for cell growth, and their synthetic nature allows control of the network's macroscopic properties and degradation mechanism. When combined with photopolymerization techniques, an aqueous cell-monomer suspension can be injected into a defect site and gelled *in situ* to form a cell-laden matrix. As an hMSC delivery vehicle for bone regeneration, the hydrogel must (i) maintain hMSC viability and permit proliferation, (ii) provide local cues that promote osteogenic differentiation, and (iii) degrade at a rate that supports the elaboration of a mineralized extracellular matrix by the delivered cells.

In general, the viability of anchorage-dependent hMSCs encapsulated in hydrogels decreases significantly with culture time due to the lack of important cell-matrix interactions. For example, in PEG-based gels, the viability of hMSCs drops to less than 15% after only one week of culture, but cell survival can be rescued by incorporation of epitopes that promote cell interactions, such as RGD^{5, 14, 15}, or functional groups that sequester cell secreted adhesion proteins, such as osteopontin^{3, 5}. Beyond providing a microenvironment that permits cell viability and proliferation, hMSC differentiation to osteoblasts within gels can be achieved by incorporation of osteogenic signaling molecules within the network. For example, growth factor loaded microparticles are often embedded in gels to provide a localized and sustained release of proteins¹⁶. In an alternative approach, dexamethasone was incorporated into PEG hydrogels through hydrolytically cleavable pendant groups, and hMSCs encapsulated within these dexamethasone-releasing PEG hydrogels differentiated to osteoblasts *in vitro* in 2 weeks¹⁷.

While important advances have been made in designing gels that promote hMSC viability and differentiation, less is known about the influence of gel degradation and temporal changes in the gel structure on tissue evolution. Here, we use a macromolecular monomer based on tri-block copolymers of poly(lactic acid)-b-PEG-b-poly(lactic acid) or polycaprolactone-b-PEG-b-polycaprolactone to synthesize gels with varying degradation profiles. To control the network degradation, the chemistry and number of degradable repeat units in the crosslinker was varied, with poly(lactic acid) repeats of 0, 2, 4, 6, 8, or 10 and poly(caprolactone) repeats of 2. To characterize the gel degradation behavior, the equilibrium water content was monitored and related to the hydrolysis of the gel crosslinks, and this information was used in a statistical-kinetic model to predict mass loss. To understand the effects of dynamic changes in the gel's macroscopic properties and mass loss on cell function, hMSCs were encapsulated in gels with varying degradation profiles, and hMSC proliferation and activity, expression of osteogenic genes, and mineralization of the gels were monitored.

10.2. MATERIALS AND METHODS

All chemicals were obtained from Sigma-Aldrich (St. Louis, MO) unless otherwise specified. All hydrogel samples were synthesized and characterized in triplicate, and error is represented as the standard deviation.

10.2.1. Macromer synthesis

The tri-block copolymers, poly(lactic acid)-b-poly(ethylene glycol)-b-poly(lactic acid) (PEG4600-nLac) were synthesized as described elsewhere¹⁸. Briefly, poly(ethylene glycol) ($M_n \sim 4600$ g/mol) was added to a 50-mL round bottom flask with a stir bar and combined with stoichiometric amounts of D,L-lactide (Polysciences) for the desired number of poly(lactic acid) repeating units. The components were melted at 140°C and purged with argon for 10 minutes, and 4.4 mg stannous octoate was added to the flask. The reaction was allowed to proceed for 4 hours at 140°C. The product was then dissolved in 20 mL CH_2Cl_2 (Fisher Scientific), precipitated three times in 200 mL ice-cold ethyl ether (Fisher Scientific), filtered, dried under vacuum, and stored at 4°C until use. PEG4600 and PEG4600-nLac macromolecular monomers were synthesized through the addition of methacrylate endgroups using a microwave-methacrylation procedure developed by Lin-Gibson *et al.* (2004)¹⁹. PEG4600-nLac or PEG4600 was placed in a microwave-resistant glass vial and purged with argon. The vial was sealed, and the contents were microwaved at 400W power for 5 minutes until molten. Methacrylic anhydride was then added to the glass vial; the vial was sealed, microwaved at 400W for 5 minutes, and cooled for 10 minutes at room temperature. The contents were microwaved again for 5 minutes. Finally, the vial was allowed to cool, and 5 mL CH_2Cl_2 was added. The product was precipitated three times in ice-cold ethyl ether, filtered, and dried under vacuum. Proton nuclear magnetic resonance ($^1\text{H-NMR}$) spectroscopy (500 MHz) was used to characterize the number of lactides added to the PEG4600 and to verify methacrylation. The ratio of lactide methyl group protons to ester PEG protons was used to determine the average amount of lactide groups per PEG molecule, and the ratio of methacrylate protons to ester PEG protons was used to verify methacrylation. PEG4600-2Cap-DMA was synthesized similarly to PEG4600-nLac-DMA, but ϵ -caprolactone was used in place of D,L-lactide. The chemical structures of PEG4600DMA, PEG4600-nLac-DMA, and PEG4600-2Cap-DMA are shown in Figure 10.1, and the NMR-verified number of degradable repeats (lactic acid or caprolactone) is reported in Table 10.1.

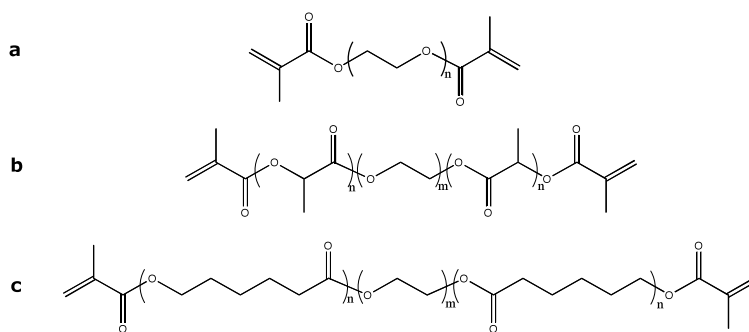


Figure 10.1. Chemical structures of the PEG-based non-degradable and degradable macromers: (a) PEG4600DMA, (b) PEG4600-nLac-DMA, and (c) PEG4600-nCap-DMA.

Table 10.1. Degradable PEG-based macromers containing varying numbers of lactic acid or caprolactone repeat units were synthesized. ¹H-NMR spectroscopy was used to determine the length of the degradable blocks (n) and to verify that methacrylation efficiency was >90%.

Product	Theoretical n	Actual n
PEG4600-2Lac-DMA	2	1.80
PEG4600-4Lac-DMA	4	3.57
PEG4600-6Lac-DMA	6	5.49
PEG4600-8Lac-DMA	8	7.77
PEG4600-10Lac-DMA	10	10.22
PEG4600-2Cap-DMA	2	1.84

10.2.2. Hydrogel synthesis and characterization

Hydrogel disks (5 mm in diameter, 2 mm in thickness) were fabricated using a solution based photopolymerization method. Briefly, 10 wt% of PEG4600-nLac-DMA or PEG4600-2Cap-DMA were dissolved in phosphate buffered saline (PBS), with 0.05 wt% of 2-hydroxy-1-[4-(hydroxyethoxy) phenyl]-2-methyl-1-propanone (I2959, Ceiba-Geigy) as a photoinitiator. The solutions were exposed to approximately 5 mW/cm² of 365 nm ultraviolet light (UVP, model XX-20) for 10 minutes²⁰. For mass loss studies, the resulting hydrogels were degraded at 37°C in PBS, and at various time points, the gels were weighed, frozen, lyophilized, and weighed again. The mass swelling ratio was then calculated for each gel by dividing the equilibrium wet mass by the dry mass²¹.

10.2.3. Human mesenchymal stem cell culture and encapsulation

Human mesenchymal stem cells were obtained from Cambrex Biosciences (Walkersville, MD) and cultured in low glucose Dulbecco's modified eagle medium (Gibco) supplemented with 10% fetal bovine serum (Invitrogen), 1% penicillin/streptomycin (Gibco), 0.25% gentamicin (Gibco), and 0.25% fungizone (Gibco), hereafter referred to as CON media. Cells that had been passaged twice were used for encapsulations.

When confluent, hMSCs were trypsinized and centrifuged to collect the cells. Each cell pellet was then mixed with a 10-wt% PEG4600-nLac-DMA macromer solution and adjusted so that the final cell concentration in the hydrogels was 25 million cells/mL. The cell/macromer suspension was mixed carefully to minimize bubble formation, and then 40 μ l of cell/macromer suspension was pipetted into 1-mL sterile syringes that had the tips cut off. The cell/macromer suspensions were then photopolymerized for 10 minutes (365 nm, 5 mW/cm²). Upon polymerization, disks were pushed out of the syringe using the plunger, placed in hMSC media (CON), and cultured at 37°C with 5% CO₂. Disks were approximately 5 mm in diameter with a thickness of 2 mm. In addition, the effect of the weight percent of macromer in solution was investigated (i.e., 8 wt%, 12 wt%, 15 wt%, 20 wt%, etc.). Cells were also photoencapsulated in non-degrading PEG4600-DMA (n=0). In some instances, gels were cultured in osteogenic differentiation media (OST, CON media supplemented with 100 nM dexamethasone, 0.05 mM ascorbic acid phosphate, and 10 mM β -glycerophosphate).

10.2.4. Biochemical analysis of encapsulated hMSCs

At days 4 and 7, cell/hydrogel constructs were removed from culture; the constructs were rinsed three times with PBS; 1 ml of PBS was added; and the samples were manually homogenized and sonicated (Model W-380, Misonix, Inc., Farmingdale, NY) for 1 minute. Alkaline phosphatase (ALP) production was measured using an assay based on the change in absorbance of *o*-nitrophenol as it is enzymatically cleaved by ALP. When ALP is present, the substrate solution undergoes a change from colorless to yellow, which can be measured at 405 nm using a spectrophotometer. The assay was performed by combining 100 μ l of sample with 100 μ l of the ALP substrate. At 5-minute intervals, the absorbance at 405 nm was measured; absorbance versus time was a straight line, the slope of which is directly proportional to the concentration of ALP. By performing the assay using known concentrations of ALP in parallel with the samples, the concentrations of ALP for the samples were calculated. To normalize alkaline phosphatase production to a relative measure of cell number (DNA content), total DNA of the samples was determined using the PicoGreen assay (Molecular Probes), and the sonicated solutions described above. Alkaline phosphatase production is presented as alkaline phosphatase per nanogram of DNA.

10.2.5. Mineralization of hydrogels by encapsulated hMSCs

Gels containing photoencapsulated hMSCs were assessed for calcium content at 4 and 7 days. Cell/hydrogel constructs were removed from culture, rinsed three times with PBS, and placed in 1 mL 0.9 N H₂SO₄ (Fisher Scientific) overnight at 4°C. The next day, 2 μ l of the supernatant was combined with 8 μ l dH₂O, and this solution was added to 100 μ l of a solution containing 1 part calcium binding reagent (0.024% *o*-cresolphthalein complexone and 0.25% 8-hydroxyquinone in dH₂O) and 1 part calcium buffer (500 mmol/L 2-amino-2-methyl-1,3 propanediol in dH₂O). The absorbance of each solution was then measured at 560 nm using a plate reader, and based on a standard curve of known concentrations of calcium chloride, the total amount of calcium deposited in each hydrogel was determined.

10.2.6. Gene expression of encapsulated hMSCs

The gene expression of encapsulated hMSCs for the extracellular matrix proteins osteopontin and collagen type I, indicators of osteogenic differentiation, was assessed using real-time reverse transcription polymerase chain reaction (RT-PCR) in both non-degradable (PEG4600DMA) and degradable (PEG4600-nLac-DMA) gels. After 1 week in culture, cell/polymer hydrogel constructs were removed from culture and rinsed three times with PBS. Total RNA was isolated using a guanidinium thiocyanate/phenol reagent (TRI reagent) and standard manufacturer's protocols. After allowing the RNA pellet to dry, it was resuspended in nuclease-free water, and any residual genomic DNA in the samples was digested (DNase I, Invitrogen). RNA was then quantified using the RiboGreen assay (Molecular Probes) based on the manufacturer's instructions.

Reverse transcription was performed using the iScript cDNA Synthesis Kit (Bio-Rad). A 10-ng total RNA sample was used for the single strand cDNA synthesis. The

reverse transcription reaction was incubated at 25 °C for 5 min, 42 °C for 30 min, and terminated at 85 °C for 5 min. PCR was conducted using the iCycler Real-Time PCR machine (Bio-Rad), and primers and probes were designed using the Beacon Designer primer design program (Table 10.2). Primers and probes (Integrated DNA Technologies) for osteopontin (OPN), collagen type I (COL I), and glyceraldehyde-3-phosphate dehydrogenase (GAPDH) were used in a multiplex format. The following PCR parameters were utilized: 95 °C for 90 sec followed by 45 cycles of 95 °C for 30 sec and 55 °C for 60 sec. Threshold cycle (C_T) analysis was used to quantify PCR products, normalized to GAPDH.

Table 10.2 a & b. (a) Forward (FWD) and reverse (REV) primers for genes assayed using real time RT-PCR. (b) Probe sequences, 5' end-labeled fluorophores, and 3' end-labeled quenchers used in real-time RT-PCR. The primers and probes could be multiplexed in the same reaction tube. Quenchers are Black Hole Quenchers (BHQ) produced by IDT Technologies.

a	Gene	FWD primer (5', 3')	REV primer (5', 3')
	OPN	ATTCTGGGAGGGCTTGGTTG	TCTGGTCCCGACGATGCT
	COL1	GGGCAAGACAGTGATTGAATACA	GGATGGAGGGAGTTTACAGGAA
	GAPDH	GCAAGAGCACAAGAGGAAGAG	AAGGGGTCTACATGGCAACT

b	Gene	Probe sequence (5', 3')	Fluorophore	Quencher
	OPN	CTCTGCCTCCTCCTGCTGCTGCTG	Texas Red X	BHQ-2
	COL1	CCAAGTCCTCCCGCCTGCCCATC	Cy5	BHQ-2
	GAPDH	ACCCTCACTGCTGGGGAGTCC	6-FAM	BHQ-1

10.3. RESULTS & DISCUSSION

10.3.1. Hydrogel characterization

The degradation behavior of gels synthesized from the PEG4600-nLac-DMA monomer was studied by following changes in the mass swelling ratio with time, and the results are shown in Figure 10.2. For all of the gel compositions studied, the initial water content was greater than 85%, which is typical for these PEG-based systems²². Because of the high water content, hydrolysis of the crosslinks is uniform throughout the gel and follows pseudo-first order reaction kinetics. Which means that the crosslinking density, ρ_{xl} , exponentially decreases with time as given below:

$$\rho_{xl} = \rho_{xlo} e^{-2nk't} \quad (\text{Equation 1})$$

Here, ρ_{xlo} is the initial crosslinking density; k' is the pseudo first order hydrolysis kinetic constant for the lactide bond; n is the number of lactide bonds in the PLA block; t is the degradation time; and the factor of 2 arises from the fact that cleavage of the PLA block on either side of the PEG breaks the crosslink. While not reported here, a similar analysis for the PEG4600-2Cap-DMA gels has been undertaken.

For highly swollen gels, the equilibrium volume swelling ratio scales with the gel crosslinking density (ρ_{xl}) to the -3/5ths power²³, which means that the volume swelling ratio for bulk degrading gels should exponentially increase with time. The solid lines in Figure 10.2 are exponential fits to the experimentally measured mass swelling ratio with time. If one assumes constant density with degradation (e.g., approximately that of wa-

ter), these gels appear to behave similarly to classic bulk degrading gels. Note that the deviations at later time points relate to changes in the gel chemistry at high extents of degradation, where the initially neutral gels become charged. In addition, the mass-swelling ratio increases at a faster rate for gels with longer PLA blocks in the crosslinks, as expected by the stoichiometry (i.e., n), and the degradation rate constant, k' , was determined to be $4.13 \times 10^{-6} \text{ min}^{-1}$. The value of understanding the degradation mechanism and determining degradation rate constant (k') is that numerous gel properties depend on the gel crosslinking density (e.g., diffusion, modulus, and others), and measuring one property can allow prediction of temporal changes in other properties²⁴.

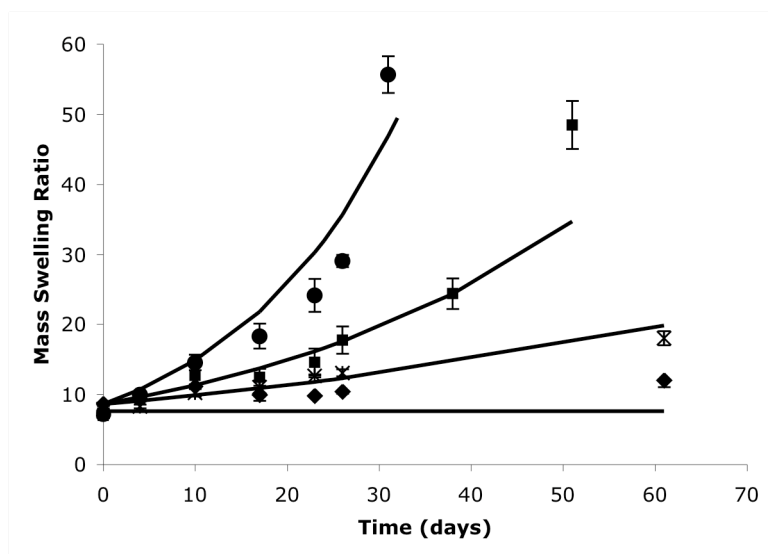


Figure 10.2. Degradation behavior of hydrogels made from PEG4600-nLac-DMA: $n=8$ (●), $n=4$ (■), $n=2$ (×), and $n=0$ (◆). As ester bonds of PEG4600-nLac-DMA hydrolyze, the gel swells; as a result, the mass swelling ratio increases. At reverse gelation, the hydrogel becomes completely soluble, and the mass swelling ratio goes to infinity. The rate of degradation is greatest when $n=8$ and is the lowest when $n=2$. When there are no degradable lactide bonds present (PEG-nLac-4600 $n=0$), degradation is negligible under these *in vitro* experimental conditions. The degradation rate constant, k' , for a poly(lactic acid) repeat unit was determined to be $4.13 \times 10^{-6} \text{ min}^{-1}$ and was used to predict the mass swelling ratio for each experimentally determined n , the solid lines on the above plot.

Of particular interest for many tissue engineering applications is understanding how mass loss occurs in biomaterial scaffolds and then manipulating the mass loss profile to support extracellular matrix deposition. Gel mass loss depends not only on the degradation kinetic constant, but also the overall connectivity of the macromolecules comprising the network. In the PEG-nLac-DMA gels studied here, the PEG molecules are connected to the network by two PLA blocks. In addition, polymerization through the methacrylate end groups leads to longer macromolecular kinetic chains that are linked to the network by numerous PEG crosslinks. One approach to understand, predict, and manipulate the gel mass loss profiles is to use statistical models to calculate the probability that the macromolecules are attached to the gel versus releasable. These models are described in detail elsewhere²⁵, but briefly, the basic equations depend upon three parameters: the hydrolysis kinetic constant (k'), the weight fraction of the network that resides in the

crosslinks versus the kinetic chains, and the network connectivity of the macromolecules, which for PEG is 2 and for the kinetic chains is N in an ideal gel.

Figure 10.3 plots the predicted gel mass loss as a function of degradation time for a series of PEG- n Lac-DMA gels, using the hydrolysis kinetic constant determined from the mass-swelling ratio. The kinetic chain connectivity, N , was determined by analysis of the time to complete dissolution of the gel, termed the reverse gel point. At the reverse gel point, fewer than two links exist per kinetic chain²⁵, and an estimate of the initial N can be determined. Here, N was fixed to 23 for all gel formulations, based on a fit of the reverse gel point. The general shape of the mass loss profile follows a slow, but steady loss of mass, which relates to the release of the PEG molecules as the PLA blocks are cleaved. Typically, >95% of the gel mass resides in the PEG molecules. The rate of this initial release depends strongly on the length of the PLA blocks. At later stages of degradation, a significant number of PLA blocks have degraded, and the kinetic chains, which are linked to the gels many times ($N=23$), begin to release. This region is shortly followed by the reverse gel point where the system transitions from an insoluble, crosslinked gel to a collection of soluble, highly-branched polymer chains. The trends in the mass loss profiles and time to complete degradation are supported by the experimental data presented in Table 10.3.

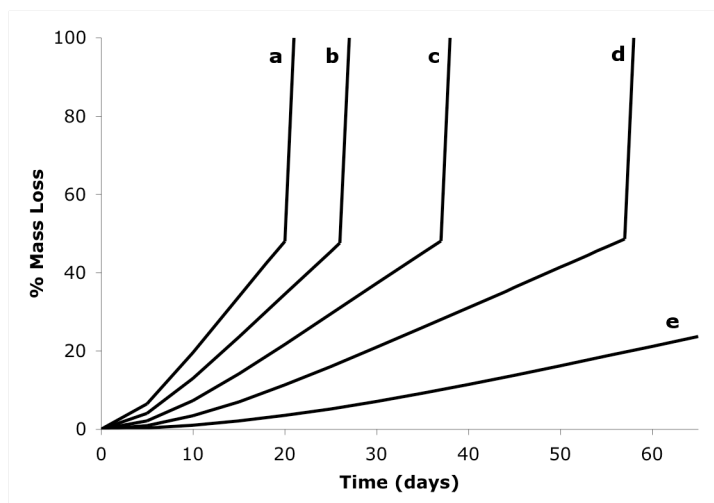


Figure 10.3. A statistical-kinetic model²⁵ was used to predict mass loss over time for the PEG4600- n Lac-DMA gels with (a) $n=10$, (b) $n=8$, (c) $n=6$, (d) $n=4$, and (e) $n=2$ lactic acid repeat units. Since all gels were processed using similar polymerization conditions and the macromers have similar molecular weights, the kinetic chain length, N , should be the approximately same for each gel while the degradation rate increases proportionally with n . The model accurately predicts trends in this behavior and the complete degradation time for gels with $n=2, 4, 6, 8$, and 10 and $N=23$.

Table 10.3. Complete degradation times of PEG4600-nLac-DMA and PEG4600-2Cap-DMA hydrogels (i.e., when the gels have completely solubilized).

Gel composition (10 wt% macromer)	Time for complete degradation	
	Observed	Predicted
PEG4600-2Lac-DMA	>62 days	>62 days
PEG4600-4Lac-DMA	51 days	58 days
PEG4600-6Lac-DMA	45 days	38 days
PEG4600-8Lac-DMA	31 days	27 days
PEG4600-10Lac-DMA	26 days	21 days
PEG4600-2Cap-DMA	>4 months	—

10.3.2. Human mesenchymal stem cell encapsulation and proliferation

The temporal changes in the network structure described above directly influence hMSC proliferation and interaction with the hydrogel matrix. For example, Figure 10.4 shows the DNA content when hMSCs were photoencapsulated at the same initial cell seeding density (25×10^6 cells/mL) in non-degrading (PEG4600DMA) and degrading (PEG4600-4Lac-DMA and PEG4600-2Cap-DMA) hydrogels up to 14 days of culture in hMSC media (CON). The DNA content increases over three-fold after only 7 days in culture in the PEG4600-4Lac-DMA hydrogels. This is in stark contrast to the non-degrading and slowly degrading gels where proliferation is restricted by the gel microstructure.

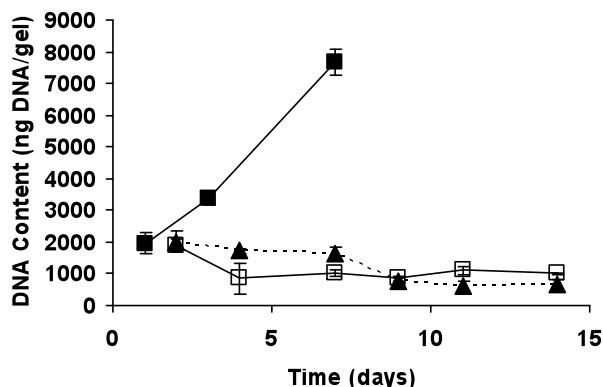


Figure 10.4. Human MSCs were photoencapsulated in non-degrading PEG4600DMA hydrogels (▲ and dotted line), PEG4600-2Cap-DMA hydrogels (□ and solid line), and PEG4600-4Lac-DMA hydrogels (■ and solid line) at a concentration of 25×10^6 cells/mL, and gels were cultured in hMSC media. DNA content (in triplicate) was measured after 7 days using the PicoGreen assay. As can be seen, DNA content increases in the PEG4600-4Lac-DMA gels, indicating that the cells are able to proliferate as gel degradation occurs.

During degradation, the gel is initially at its highest crosslinking density, and there is little room for cells to spread out and extend processes. Over time, ester bonds gradually

hydrolyze. At some point, the gel is sufficiently degraded and the pore size is large enough that hMSCs are able to extend processes, spread out, and proliferate (as shown in Figure 10.4). Other groups have studied MSCs encapsulated in degradable [poly(ethylene glycol) fumarate] gels³. Unlike our results, where we saw high proliferation of hMSCs initially, Temenoff *et al.* (2004)³ saw no evidence of rat MSC proliferation after encapsulation in oligo[poly(ethylene glycol) fumarate] hydrogels. This may be related to differences in the cell type.

10.3.3. Biochemical activity of encapsulated hMSCs

Figure 10.5 A shows the results of alkaline phosphatase activity assays conducted on PEG4600DMA and PEG4600-4Lac-DMA hydrogels containing photoencapsulated hMSCs and cultured in either CON or OST media. In all cases, ALP activity decreased from day 4 to day 7. Alkaline phosphatase is thought to aid in nucleation of mineral formation by removing nucleation inhibitors²⁶. Increased expression of alkaline phosphatase by hMSCs usually indicates osteogenic differentiation. In developing osteoblasts, alkaline phosphatase activity disappears when the cells become embedded in the matrix as osteocytes²⁷. Since there is already a matrix-like material (i.e., the PEG scaffold) present when hMSCs are encapsulated, we hypothesize that elevated alkaline phosphatase activity is not needed. Alkaline phosphatase is responsible for the initiation of matrix mineralization. It is possible that nucleation of mineral formation occurs quickly in these scaffolds, and since nucleation is already occurring in the gels, the cells decrease synthesis of alkaline phosphatase since it is simply not needed for nucleation or mineralization of the surrounding matrix. This would explain the decrease in ALP activity with time in all samples. However, alkaline phosphatase activity is likely modulated by two factors in PEG hydrogels: matrix-like interactions acting at the cell membrane that tend to down-regulate ALP expression and increases in ALP expression due to molecular changes brought about in response to the osteogenic differentiation media (i.e., dexamethasone stimulates the up-regulation of osteogenic genes, such as ALP).

10.3.4. Mineralization of Hydrogels by encapsulated hMSCs

The ability of cells encapsulated in PEG4600-4Lac-DMA hydrogels to mineralize with time was assessed using an assay specific to calcium. Human MSCs were photoencapsulated in these hydrogels, and they were cultured in either CON or OST media. After 4 and 7 days, calcium content was measured, and the results are shown in Figure 10.5 B.

After 4 days, there is much greater mineralization in the degradable gels cultured in OST media than non-degradable gels cultured in either media or degradable gels cultured in CON media. After 7 days, the non-degradable gels are beginning to mineralize, which is consistent with our previously published results⁵. It has been shown that mineralization of polymers can be greatly enhanced by the presence of carboxylic acid groups^{28, 29}. Hydrolysis of the lactide ester bonds yields a hydroxyl group and a carboxylic acid group. One reason for increased mineralization in the degradable hydrogels cultured in OST media may be due to increased presence of carboxylic acid groups upon hydrogel degradation. However, if this were the case (i.e., carboxylic acid groups lead to mineralization), one would also expect high mineralization in the gels cultured in CON media

since carboxylic acid groups are also being generated upon degradation in these gels. The β -glycerophosphate present in OST media acts as a mineralization nucleator and probably contributes to the increased mineralization that is seen over constructs cultured in CON media.

An alternative explanation is that gel-encapsulated hMSCs are differentiating to the osteoblastic lineage in response to dexamethasone present in OST media. As a result, alkaline phosphatase activity increases and causes an increase in mineralization. However, the results of alkaline phosphatase activity assays disprove this hypothesis. Therefore, it is likely that the combined effects of β -glycerophosphate present in OST media and the carboxylic acid groups generated during gel degradation lead to increased mineralization in degradable hydrogels cultured in OST media.

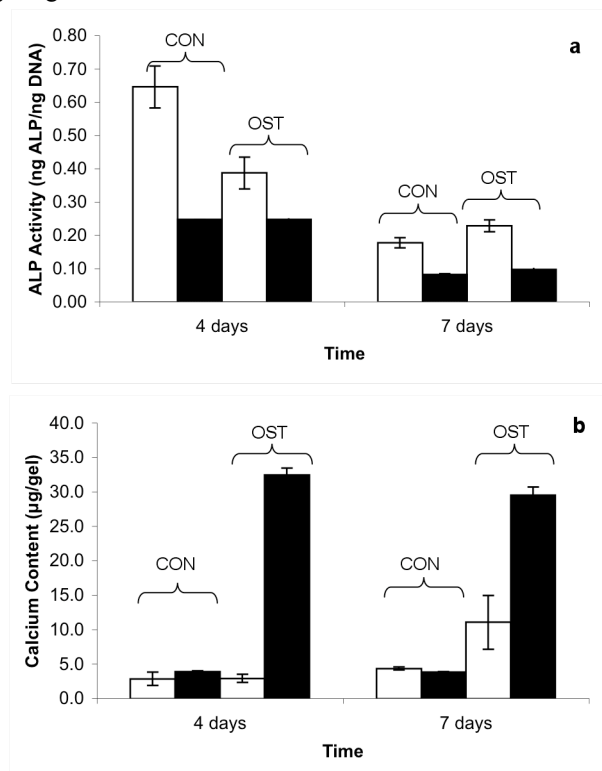


Figure 10.5 a & b.

(a) Human MSCs were photoencapsulated in PEG4600DMA hydrogels (non-degrading) and PEG4600-4Lac-DMA hydrogels (degrading), and gels were cultured in either control media (CON) or osteogenic differentiation media (OST). After 4 and 7 days in culture, alkaline phosphatase (ALP) activity was assessed and normalized to DNA: non-degradable gels cultured in CON media and OST media (white bars) and degradable gels cultured in CON media and OST media (black bars). ALP activity drops between day 4 and 7 in all samples, and ALP activity is higher in non-degradable gels than degradable gels cultured in the same media.

(b) Human MSCs were photoencapsulated as described in (a). After 4 and 7 days in culture, total calcium that had been deposited was measured using a calcium binding assay: non-degradable gels cultured in CON media and OST media (white bars) and degradable gels cultured in CON media and OST media (black bars). The rate of mineralization of degrading hydrogels was much faster ($\sim 10\times$) than non-degrading hydrogels. The high rate of mineralization was likely due to the formation of acidic groups within the hydrogel that form during ester hydrolysis.

10.3.5. Gene expression of encapsulated hMSCs

When hMSCs are encapsulated in the PEG hydrogel, the surrounding environment is foreign (i.e., no cellularly-recognized extracellular matrix *per se*). To respond to this foreign environment, the cells must produce their own matrix proteins; for bone matrix these are mainly collagen type I (COL1) and the adhesion protein osteopontin (OPN). OPN is implicated in general cell attachment to the extracellular matrix (ECM) by osteoprogenitor cells, such as MSCs³⁰. To alter the hydrogel environment to a more native environment (i.e., containing recognizable ECM proteins), the cells must synthesize and secrete ECM components, such as OPN and COL1. Figure 10.6 A shows the gene expression of OPN as a function of scaffold composition (i.e., non-degradable vs. degradable) and media composition (control media or osteogenic differentiation media) as measured using real-time RT-PCR.

First, there is a large difference between gene expression of OPN in CON media and OST media in non-degradable gels. The dexamethasone in OST media generally leads to an increase in osteogenic genes, one of which is OPN. However, in Figure 10.6 A it is apparent that the gene expression of OPN is greater in both non-degradable and degradable gels when culture in CON media than in OST media. When cultured in OST media, the β -glycerophosphate present leads to mineralization in the gel⁵. We hypothesize that this mineralization within the gel leads to sequestering of osteopontin within the hydrogel; therefore, cells encapsulated in the hydrogel and cultured in OST media would need to produce less OPN in order to adhere to the gel since any secreted OPN would more readily adsorb to the mineralized extracellular hydrogel environment. In contrast, cells in gels cultured in CON media need to produce extremely high levels of OPN to adhere to the extracellular hydrogel network since the secreted OPN does not adsorb well due to lack of mineral regions throughout the gel. This hypothesis is further supported by results published elsewhere⁵.

However, in degradable gels the gene expression of OPN when the gels are cultured in CON media is much greater (5.3 in degradable gels as compared to 1.2 in non-degradable gels). This may be explained by the fact that these hydrogels are quickly degrading, and mass loss continues to increase with time. The cells need to produce increasing amounts of OPN in order to adhere to the non-mineralized gels. Interestingly, the gene expression of OPN in degradable gels cultured in OST media is much lower than the same gels cultured in CON media. This is likely due to mineralization occurring in these degradable gels cultured in OST media. In fact, the low OPN gene expression observed in both non-degradable and degradable hydrogels cultured in OST media may be directly related to the high mineralization seen in these same gels (see Figure 10.5 B).

Figure 10.6 B shows the gene expression of collagen type I in the same samples as Figure 10.6 A. We hypothesize that two factors govern the gene expression of COL1 in PEG hydrogels. First, COL1 expression can be up-regulated by osteogenic differentiation media. This is seen when comparing non-degradable gels cultured in CON media vs. OST media in Figure 10.6 B. The dexamethasone in OST media leads to up-regulation of osteogenic genes, and COL1 is a gene implicated in osteogenic differentiation of hMSCs. Second, we believe there is another component that regulates COL1 expression, which is implicated in the general hMSC surrounding extracellular matrix environment. According to our hypothesis, as the synthetic matrix is eroded, the hMSCs up-regulate the gene expression of COL1 in order to synthesize their own matrix for cell attachment, etc. Alternatively, since the synthetic matrix is quickly eroding away, this stimulates the

production of more matrix material by the encapsulated hMSCs, leading to an even greater COL1 gene expression. In fact, COL1 gene expression is significantly higher in the degradable gels as compared to the non-degradable gels in both CON and OST media.

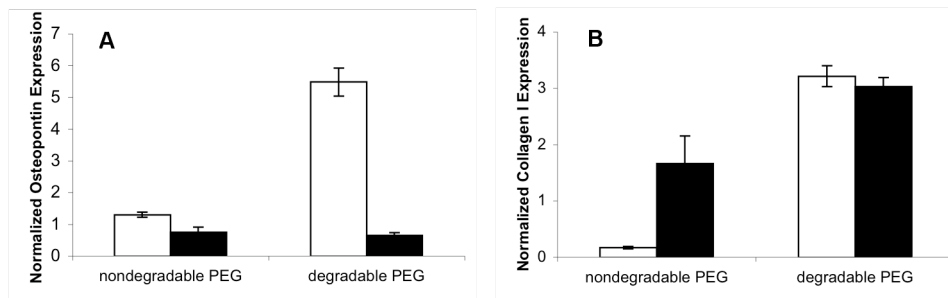


Figure 10.6 A & B.

(A) Gene expression of osteopontin was measured by real-time RT-PCR. Human MSCs were photoencapsulated in non-degradable hydrogels (PEG4600DMA) and degradable hydrogels (PEG4600-4Lac-DMA) and cultured in either CON media (white bars) or OST media (black bars) for 7 days. Gene expression was normalized to gene expression of glyceraldehyde-3-phosphate dehydrogenase.

(B) Gene expression of collagen type I was measured by real-time RT-PCR. Human MSCs were photoencapsulated in non-degradable hydrogels (PEG4600DMA) and degradable hydrogels (PEG4600-4Lac-DMA) and cultured in either CON media (white bars) or OST media (black bars). Gene expression was normalized to gene expression of glyceraldehyde-3-phosphate dehydrogenase.

10.4. CONCLUSIONS

Hydrogel degradation can be controlled by incorporation of hydrolytically labile bonds within a PEG crosslinker: poly(lactic acid) blocks for fast degradation or polycaprolactone blocks for slow degradation. Degradation of the network can be accurately predicted by a statistical-kinetic model and utilized to control gel properties for tailored cell-matrix interactions. Degradable hydrogels of PEG4600-4Lac-DMA allowed proliferation of encapsulated hMSCs, while hMSCs encapsulated in nondegradable or slowly-degradable hydrogels of PEG4600-DMA exhibited negligible proliferation over the same time period. The biochemical activity and gene expression of the encapsulated hMSCs were characterized as a function of the gel chemistry. Cellular response to the temporally changing network structure in different culture conditions, CON or OST media, was complex. Due to the presence of β -glycerophosphate and increased carboxylic acid groups within the network, increased mineralization of degradable gels in OST media was observed, which in turn decreased ALP activity and OPN gene expression as the hMSCs were able to interact with the mineralized matrix. Increased COL1 gene expression was observed in nondegradable gels in OST media, which indicates osteogenic differentiation, as well as in degradable gels in both CON or OST media.

10.5. ACKNOWLEDGMENTS

The authors would like to acknowledge the Howard Hughes Medical Institute and National Institutes of Health (DE16523) for research funding, the National Science Foundation and Department of Education's Graduate Assistantships in Areas of National Need (GAANN) for graduate research fellowships to CRN, and the National Aeronautics and Space Administration's Graduate Student Research Program (NASA GSRP) and GAANN for graduate research fellowships to AMK.

10.6. REFERENCES

1. K. Al-Hamdan, R. Eber, D. Sarment, C. Kowalski, H. L. Wang, Guided tissue regeneration-based root coverage: Meta-analysis, *J. Periodont.* **74**(10), 1520-1533 (2003).
2. L. Laurell, J. Gottlow, M. Zybutz, R. Persson, Treatment of intrabony defects by different surgical procedures. A literature review, *J. Periodont.* **69**(3), 303-313 (1998).
3. J. S. Temenoff, H. Park, E. Jabbari, T. L. Sheffield, R. G. LeBaron, C. G. Ambrose, A. G. Mikos, In vitro osteogenic differentiation of marrow stromal cells encapsulated in biodegradable hydrogels, *J. Biomed. Mater. Res. Part A* **70A**(2), 235-244 (2004).
4. B. Sharma, J. H. Elisseeff, Engineering structurally organized cartilage and bone tissues, *Ann. Biomed. Eng.* **32**(1), 148-159 (2004).
5. C. R. Nuttelman, M. C. Tripodi, K. S. Anseth, Synthetic hydrogel niches that promote hMSC viability, *Matrix Biol.* **24**(3), 208-218 (2005).
6. C. B. Ballas, S. P. Zielske, S. L. Gerson, Adult bone marrow stem cells for cell and gene therapies: Implications for greater use, *J. Cell. Biochem.* **38**(Supplement), 20-28 (2002).
7. A. I. Caplan, Mesenchymal Stem-Cells, *J. Orthop. Res.* **9**(5), 641-650 (1991).
8. S. E. Haynesworth, M. A. Baber, A. I. Caplan, Cell-Surface Antigens On Human Marrow-Derived Mesenchymal Cells Are Detected By Monoclonal-Antibodies, *Bone* **13**(1), 69-80 (1992).
9. M. F. Pittenger, A. M. Mackay, S. C. Beck, R. K. Jaiswal, R. Douglas, J. D. Mosca, M. A. Moorman, D. W. Simonetti, S. Craig, D. R. Marshak, Multilineage potential of adult human mesenchymal stem cells, *Science* **284**(5411), 143-147 (1999).
10. L. Wang, R. M. Shelton, P. R. Cooper, M. Lawson, J. T. Triffitt, J. E. Barralet, Evaluation of sodium alginate for bone marrow cell tissue engineering, *Biomaterials* **24**(20), 3475-3481 (2003).
11. W. J. Li, R. Tuli, C. Okafor, A. Derfoul, K. G. Danielson, D. J. Hall, R. S. Tuan, A three-dimensional nanofibrous scaffold for cartilage tissue engineering using human mesenchymal stem cells, *Biomaterials* **26**(6), 599-609 (2005).
12. W. J. Li, R. Tuli, X. X. Huang, P. Laquerriere, R. S. Tuan, Multilineage differentiation of human mesenchymal stem cells in a three-dimensional nanofibrous scaffold, *Biomaterials* **26**(25), 5158-5166 (2005).
13. H. Shin, P. Q. Ruhe, A. G. Mikos, J. A. Jansen, In vivo bone and soft tissue response to injectable, biodegradable oligo(poly(ethylene glycol) fumarate) hydrogels, *Biomaterials* **24**(19), 3201-3211 (2003).
14. H. Shin, K. Zygourakis, M. C. Farach-Carson, M. J. Yaszemski, A. G. Mikos, Modulation of differentiation and mineralization of marrow stromal cells cultured on biomimetic hydrogels modified with Arg-Gly-Asp containing peptides, *J. Biomed. Mater. Res. Part A* **69A**(3), 535-543 (2004).
15. F. Yang, C. G. Williams, D. A. Wang, H. Lee, P. N. Manson, J. Elisseeff, The effect of incorporating RGD adhesive peptide in polyethylene glycol diacrylate hydrogel on osteogenesis of bone marrow stromal cells, *Biomaterials* **26**(30), 5991-5998 (2005).
16. J. Elisseeff, W. McIntosh, K. Fu, T. Blunk, R. Langer, Controlled-release of IGF-I and TGF-beta 1 in a photopolymerizing hydrogel for cartilage tissue engineering, *J. Orthop. Res.* **19**(6), 1098-1104 (2001).
17. C. R. Nuttelman, M. C. Tripodi, K. S. Anseth, Dexamethasone-functionalized gels induce osteogenic differentiation of encapsulated hMSCs, *J. Biomed. Mater. Res.* **In Press** (2005).
18. A. S. Sawhney, C. P. Pathak, J. A. Hubbell, Bioerodible hydrogels based on photopolymerized poly(ethylene glycol)-co-poly(alpha-hydroxy acid) diacrylate macromers, *Macromolecules* **26**(4), 581-587 (1993).
19. S. Lin-Gibson, S. Bencherif, J. A. Cooper, S. J. Wetzel, J. M. Antonucci, B. M. Vogel, F. Horkay, N. R. Washburn, Synthesis and characterization of PEG dimethacrylates and their hydrogels, *Biomacromolecules* **5**(4), 1280-7 (2004).

20. S. J. Bryant, C. R. Nuttelman, K. S. Anseth, Cytocompatibility of UV and visible light photoinitiating systems on cultured NIH/3T3 fibroblasts in vitro, *J. Biomater. Sci.-Polym. Ed.* **11**(5), 439-457 (2000).
21. S. J. Bryant, K. S. Anseth, Photopolymerization of hydrogel scaffolds. In *Scaffolding in Tissue Engineering*, J. Elisseeff, P. X. Ma, Eds. Marcel Dekker, Inc.: Vol. In Press.
22. A. T. Metters, K. S. Anseth, C. N. Bowman, Fundamental studies of a novel, biodegradable PEG-b-PLA hydrogel, *Polymer* **41**(11), 3993-4004 (2000).
23. A. T. Metters, C. N. Bowman, K. S. Anseth, Verification of scaling laws for degrading PLA-b-PEG-b-PLA hydrogels, *Aiche J.* **47**(6), 1432-1437 (2001).
24. P. Martens, A. T. Metters, K. S. Anseth, C. N. Bowman, A generalized bulk-degradation model for hydrogel networks formed from multivinyl cross-linking molecules, *J. Phys. Chem. B* **105**(22), 5131-5138 (2001).
25. A. T. Metters, C. N. Bowman, K. S. Anseth, A statistical kinetic model for the bulk degradation of PLA-b-PEG-b-PLA hydrogel networks, *J. Phys. Chem. B* **104**(30), 7043-7049 (2000).
26. V. I. Sikavitsas, J. S. Temenoff, A. G. Mikos, Biomaterials and bone mechanotransduction, *Biomaterials* **22**, 2581-2593 (2001).
27. M. Holtrop, The ultrastructure of bone, *Annals of Clinical and Laboratory Science* **5**264-271 (1975).
28. W. L. Murphy, D. J. Mooney, Bioinspired growth of crystalline carbonate apatite on biodegradable polymer substrata, *J Am Chem Soc* **124**(9), 1910-7 (2002).
29. J. Song, E. Saiz, C. R. Bertozzi, A new approach to mineralization of biocompatible hydrogel scaffolds: an efficient process toward 3-dimensional bonelike composites, *J Am Chem Soc* **125**(5), 1236-43 (2003).
30. H. Ohgushi, A. I. Caplan, Stem cell technology and bioceramics: from cell to gene engineering, *J Biomed Mater Res* **48**(6), 913-27 (1999).